



Original articles

Research article

<https://doi.org/10.17308/kcmf.2023.25/11108>

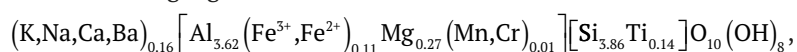
Specifying the structural formula of kaolinite from the Orenburg Region by means of spectroscopic methods

A. G. Chetverikova¹✉, V. N. Makarov¹, O. N. Kanygina¹, M. M. Seregin², E. A. Stroganova¹¹Orenburg State University,
13 Prospect Pobedy, Orenburg 460018, Russian Federation²LLC “Lumex-Centrum”
28A Varshavskoe sh., Moscow 117105, Russian Federation**Abstract**

Kaolinite certification is necessary when using it as a raw material in the ceramic industry. The kaolin clay deposit discovered in the Orenburg Region in 2018 is presumably the largest in the country. Within the Koskolskaya area, 5 mineral deposits have been described. Three of them are particularly promising deposits of high-quality kaolin clay. Previously, studies of the technological and physical characteristics of clay from this deposit were carried out. The purpose of our study was to derive and specify the structural formula of kaolinite contained in the clays.

After elutriation and grinding in a ball mill, natural clay was sifted through a sieve with meshes of 40 μm. The conducted IR, Raman, and EPR spectroscopy, as well as DTA allowed us to monitor the process of metakaolinisation, which occurs as a result of dehydration of kaolinite (i.e. the process of transformation of kaolinite into metakaolinite). Spectroscopic methods made it possible to analyse the parameters of the fine structure, in particular, the degree of crystallinity of kaolinite particles and the occurrence of iron and magnesium ions in hydroxyl sheets.

Conducting a series of experiments, we managed to specify the structural formula of the kaolinite of the Koskolsky deposit of the Orenburg region:



The square brackets indicate the cationic compositions of the hydroxyl and siloxane sheets that formed the surface charge of the mineral particles. Compensator ions remain outside the square brackets. Thus, in our study we assessed the substance used as a raw material in the ceramic industry and determined the role of elutriation and mechanical treatment of kaolin clay.

Keywords: Structure, Kaolinite, XRF spectroscopy, Differential thermal analysis, FTIR spectroscopy, Raman spectroscopy, EPR spectroscopy

Funding: This study was supported by the Russian Foundation for Basic Research and the government of the Orenburg Region (project No. 9-43-560001 r_a “Physicochemical processes of microwave consolidation of kaolinites”).

Acknowledgments: the XRF spectroscopy and the Raman spectroscopy were performed using the equipment of the Engineering Centre of Orenburg State University.

For citation: Chetverikova A. G., Makarov V. N., Kanygina O. N., Seregin M. M., Stroganova E. A. Specifying the structural formula of kaolinite from the Orenburg Region by means of spectroscopic methods. *Condensed Matter and Interphases*. 2023;25(2): 277–291. <https://doi.org/10.17308/kcmf.2023.25/11108>

Для цитирования: Четверикова А. Г., Макаров В. Н., Каныгина О. Н., Серегин М. М., Строганова Е. А. Коррекция структурной формулы каолинита Оренбургской области спектроскопическими методами. *Конденсированные среды и межфазные границы*. 2023;25(2): 277–291. <https://doi.org/10.17308/kcmf.2023.25/11108>

✉ Chetverikova Anna Gennadievna, e-mail: kr-727@mail.ru

© Chetverikova A. G., Makarov V. N., Kanygina O. N., Seregin M. M., Stroganova E. A., 2023



The content is available under Creative Commons Attribution 4.0 License.

1. Introduction

Over 3/4 of the Earth's crust consists of silicate rocks whose finely dispersed powders are used to synthesise technical ceramics [1]. Following the current trends in physical materials science, the potential of clays is determined by their key parameters, namely their chemical, mineralogical, and phase compositions. Kaolinite has long been used in ceramics, coatings, paper, and oil industries. It is now largely considered to be a promising material for the production of more valuable products that can be widely used for industrial purposes [2, 3]. Kaolinite is reported to be used for the production of materials with new physical and chemical properties [4, 5]. The phase composition of kaolin clays is important for determining their functional properties including the sorption process [6], catalysis [7], sintering [8], etc.

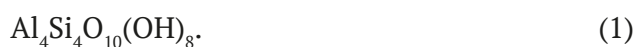
The main method used to identify the phases of crystalline minerals is X-ray diffraction. However, it does not always register poorly crystallized minerals, even when they are present in significant quantities. X-ray diffraction analysis is not sensitive enough to register small distortions in the crystal lattice caused by isomorphic substitutions, especially when their number is insignificant. Impurity phases, even in small quantities, can lead to incorrect conclusions regarding the structure of the mineral. Therefore, aluminosilicate minerals have mainly been analysed by means of spectroscopic methods, including infrared (IR) spectroscopy and electron paramagnetic resonance (EPR) spectroscopy [9, 5, 10]. Kaolin clays contain a relatively small number of paramagnetic ions. Therefore, EPR spectroscopy [11] can provide valuable information regarding the nature and distribution of paramagnetic ions in transition metals, free radicals, and structural defects [12–14], which can be important for determining the degree of conductivity.

The Orenburg Region is rich in kaolin clays. Within the Koskolskaya area, 5 mineral deposits have been described. The kaolin clay deposits found in the Orenburg Region in 2018 are presumably the largest in the Russian Federation and are of a high quality [15]. Kaolin clay mining is currently of economic strategic importance for Russia. It provides valuable information that

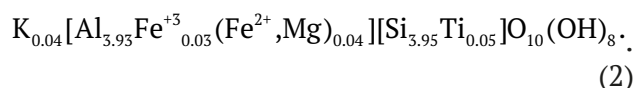
can be used to build a database of eluvial mineral deposits. Therefore, the exploration and material studies of kaolin clays in the Svetlinsky area are of utmost importance [16, 17].

Samples of kaolin were analysed in much detail in [8, 18, 19] by means of colorimetric gradation, X-ray diffraction analysis, and fractal analysis. This article presents the results of further studies of enriched kaolin and provides new information obtained by means of spectroscopic methods and derivative thermal analysis.

Kaolinite, being the main component of kaolin clay, is a layered clay mineral which belongs to the aluminosilicate group. Each layer consists of a tetrahedral (T) sheet composed of silicon and oxygen ions and an octahedral (O) sheet composed of oxygen, aluminium, and hydroxyl ions linked by hydrogen and molecular bonds (Fig. 1). The mineral has a triclinic structure (space group aP13). When the crustal lattice deteriorates, the structure can transform into monoclinic. Ideally, kaolinite does not show any isomorphism, and the structural formula is presented as follows:



The averaged structural formula of kaolinite taking into account isomorphism is presented as follows [20]:



The square brackets indicate cationic compositions of the hydroxyl (octahedral) and siloxane (tetrahedral) sheets (Fig. 1) forming the surface charge of the particles. Deriving the structural formula of the Orenburg natural kaolinite – is a difficult but important task required for the certification of the material used in industrial production.

The purpose of our study was to derive and specify the structural formula of kaolinite by means of a comprehensive analysis of enriched eluvial kaolin from the Orenburg Region deposits.

2. Experimental

2.1. Materials

In our study, we analysed samples of natural clay mined in the Orenburg Region. X-ray phase analysis demonstrated [18] that the

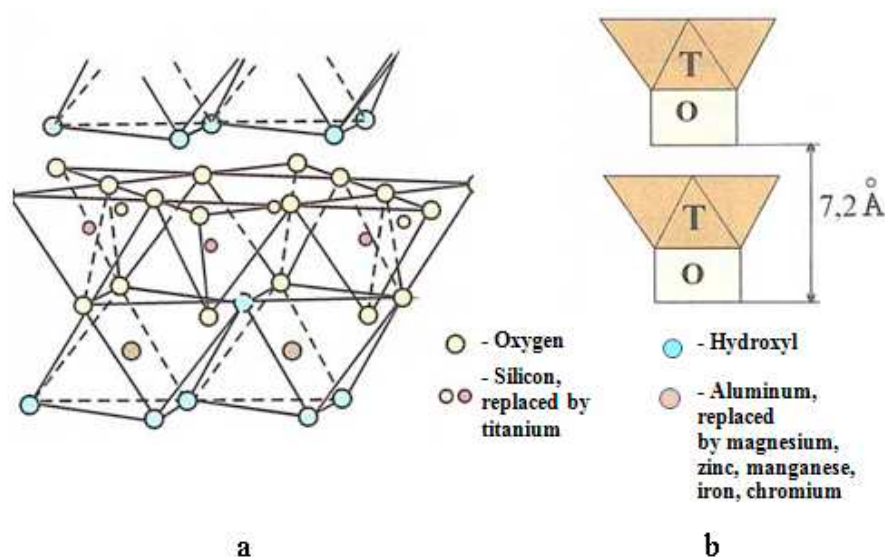
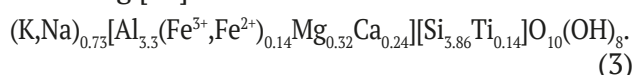


Fig. 1. Kaolinite structure: a – atomic, b – schematic [20]

clay contained about 40% (vol.) of amorphous and 60% (vol.) of crystalline modifications. Of the crystalline phases, kaolinite substituted 73.2 wt.%, corundum – 15.4 wt.%, and free silica – 11.4 wt.%. Finely dispersed clay materials have a low degree of crystallinity, i.e. they are X-ray amorphous. Therefore, the validity of the complete phase analysis of the sample is not very high.

The elemental composition of kaolin, expressed in form of oxides, was determined by means of chemical analysis according to [21]. The resulting preliminary structural formula was the following [22]:



The comparison of the structural formula (3) with the averaged formula (2) and the ideal formula (1) demonstrated that kaolinite from the studied deposit includes a large number of isomorphous substitutions and is far from ideal.

Further in the article we describe the results of the analysis of kaolin clay after mechanical treatment, namely after it was grounded in an iMold milling machine and subjected to sieve analysis with the mesh size of 40 μm .

The isoelectric point of mechanically treated kaolin clay ($d \leq 40 \mu\text{m}$) determined according to [23] is close to $\text{pH} = 2$, since the ζ -potential decreases from +5 to –20 mV, when pH decreases from 1.5 to 3.3 [24]. In proximity to the isoelectric point of the mineral cleavages, the dissociation of

silanol (Si–OH) and aluminium (Al–OH) groups was minimum, and the insignificant numbers of positive and negative charges formed on the cleavages were equal. As a result, when $\text{pH} = 2$, we managed to determine the granulometric composition of the clay by means of photon correlation spectroscopy [25]. The size of the particles is represented by three modal peaks: (0.14 ± 0.05); (1.13 ± 0.40); (23.4 ± 2.7) μm .

To study the structural state of kaolinite in mechanically treated clay in more detail we used methods which helped us to assess both mineralogical parameters (2.2–2.3) and the fine structure (methods 2.4–2.6).

2.1. X-ray fluorescence analysis (XRF)

X-ray fluorescence analysis helped us to specify the elemental composition of the kaolin clay. X-ray fluorescence spectra were recorded using a Spectroscan MAX-GVM vacuum energy-dispersive X-ray spectrometer in the wavelength range from 800 to 14000 mÅ. The analysing crystals were PET, LiF, KAP, and C002. Powder samples were pressed into 20 mm tablets on a boric acid substrate at a ratio of 5:4.

2.2. Differential thermal analysis (DTA)

Differential thermal analysis (DTA) was used to monitor structural transformations in the mechanically treated kaolin clay sample. Derivatograms were recorded using a Thermoscan-2 unit with a heating rate of 10 $^{\circ}\text{C}/\text{min}$ according to [26]. The sample was

heated from room temperature to 900 °C. The error for temperature measurement was ± 1 °C. Aluminium oxide powder (Al_2O_3) with a weight of 0.5 g and sealed in a quartz container was used as a reference. The weight of the analysed sample was 0.50 ± 0.01 g.

2.3 Optical microscopy

The morphological analysis of kaolinite particles (their size, shape, and surface properties) was conducted. The images were obtained using a Bresser optical microscope, with a CELESTRON digital camera with a resolution of 5 MP.

2.4. Infrared (IR) spectroscopy

The IR spectra of the initial and annealed (after DTA) samples were registered using an InfraLum FT-08 spectrometer (Lumex) with a potassium bromate optical system. The spectrometer had an attachment for disturbed total internal reflection (DTIR) with a zinc selenide crystal. The measurement cycle time was 120 seconds. The spectral range was from 525 to 8000 cm^{-1} with a step of 4 cm^{-1} . Before each measurement, the background spectrum of the attachment was assessed. Powder sample was then placed on the surface of the crystal under a high pressure. After each measurement the crystal was cleaned with cotton wool wetted with acetone.

2.5. Raman spectroscopy

Raman spectroscopy is used to analyse a large number of chemical substances whose molecules are active in the Raman spectra (the substance can be a solution, a solid, or in a multi-phase state) and their concentration does not exceed 0.1%. This approach is important for studying clay materials. The Raman spectra of the initial sample were registered using a RamMix M532 spectrometer. The spectral range was from 120 to 4000 cm^{-1} with a step of 4 cm^{-1} . Before each measurement, the background spectrum of the attachment was assessed. The IR spectroscopy and the Raman spectroscopy – complement each other and demonstrate bond vibrations of various intensity [27].

2.6. Electron paramagnetic resonance (EPR) spectroscopy

The sensitivity of the EPR spectroscopy depending on the type of paramagnetic centres

during a qualitative mineralogical analysis is up to $0.08 \div 0.10\%$. Some ions including Fe^{3+} , Fe^{2+} , Cu^{2+} , Mn^{2+} , and Ti^{4+} , which have unpaired electrons on *d*-sheaths, have non-zero electron spins and magnetic moments. This makes it possible to analyse the minerals containing these ions by means of electron paramagnetic resonance spectroscopy. The EPR method is gaining popularity and is used to study the fine structure of clay materials. A large number of studies are fully or partially dedicated to the interpretation of EPR spectra created by paramagnetic ions or radicals in clays [28, 29].

Besides the lines of metal ions, EPR spectra of aluminosilicates often demonstrate narrow lines of paramagnetic defects of the electron structure, namely localised unpaired electrons and holes. Both types of centres – electron and hole – have *g*-factors close to $g \approx 2.00$. It is believed [28, 30] that electron centres have $g \leq 2.00$ and hole centres have $g \geq 2.00$. Therefore, EPR spectra can provide accurate data regarding their localisation.

The EPR spectra of the initial samples and samples after DTA were registered using a CMS8400 compact automatic controlled spectrometer at room temperature. The spectra were registered under the following conditions: frequency of 9.86 GHz, magnetic field of $1 \div 7$ kOe, magnetic field modulation frequency of 100 kHz and amplitude of 6 Hz.

3. Results and discussion

3.1. Specifying the elemental composition by means of XRF

X-ray fluorescence analysis of mechanically treated kaolin clay from the Svetlinsky area of the Orenburg Region has not yet been described in literature. Table 1 presents the chemical composition of the clay expressed in form of oxides. The compositions are listed from the largest to the smallest quantitative content. The legend is given below the table. Elements whose content increased or decreased after the processing are shown in pink and blue. Trace amounts of barium, sulphur, and chromium registered by the XRF are tinted yellow. The content of paramagnetic centres (Fe_2O_3 and MnO) did not change after mechanical treatment within the experimental error. The concentration of the following oxides increased significantly: SiO_2 – by 10%, Al_2O_3 – by 20%, and MgO – by

Table 1. Composition of the enriched kaolin clay obtained by means of X-ray fluorescence analysis

SiO ₂	Al ₂ O ₃	K ₂ O	TiO ₂	MgO	Fe ₂ O ₃	BaO	SO ₂	CuO	CaO	P ₂ O ₅	MnO	Cr ₂ O ₃
59.13	27.35	7.04	2.43	2.23	1.84	0.19	0.13	0.08	0.07	0.04	0.03	0.02
Z	increased		Z	decreased		Z	hasn't changed		Z	discovered		

2 times. The concentration of CuO – decreased by 3 times, and the concentration of CaO decreased by 30 times [21].

Table 1 demonstrates that the chemical composition of the sample includes the following oxides: SiO₂ (silica), Al₂O₃ (alumina), Na₂O and K₂O (alkali oxides), Fe₂O₃ and TiO₂ (colouring oxides), as well as CaO (lime), and MgO (magnesia). Silica was found in the clays in bound (in clay minerals) and free states (in sand and quartz dust impurities). Its total content is usually about 60÷65% in clays, and up to 85% in oversanded clays. Therefore, the analysed sample was not oversanded.

The silica was found in the clay mainly in a bound state (clay minerals and mica impurities). It is a highly refractory oxide ensuring the refractoriness of clays. Based on the content of silica and titanium dioxide (%) the analysed clay was classified as semiacid [26].

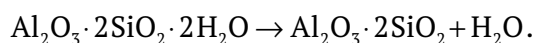
Iron oxide (1.84%) in the form of isomorphic substitutions of the ions of the hydroxyl layer practically did not have any colouring effect. Titanium dioxide (2.43%) was present in the form of isomorphic impurities in the siloxane sheet of the kaolinite lattice.

Alkali oxides, which reduce the colouring effect of iron and titanium oxides by reducing the melting point of clay, were present in the clay minerals and impurities in the isomorphic form. Their content was below 8%. High concentrations of these compounds enabled us to perform chemical processing – elutriation, i.e. removal of water-soluble salts. As a result, their concentration in the sample was below 1.5%. The percentage of crystalline kaolinite in mechanically and chemically treated clays exceeded 77% (vol.) [21].

[17] pointed out that the composition of elutriated finely dispersed kaolin clay (with low concentrations of Na and K oxides) is close to monokaolinite, which makes it a promising material for obtaining metakaolinite - an intermediate product whose areas of application are constantly extending.

3.1. Differential thermal analysis of kaolin clay

In order to study the physico-chemical processes occurring in the clay, the sample was subjected to thermal treatment at 900 °C. At this temperature, the calcination of kaolinite is usually complete and it transforms into metakaolinite [31]. The thermogram presented in Fig. 2 demonstrates an endothermic effect in the said temperature range, which started at a temperature of about 520 °C and ended at 680 °C. Maximum energy absorption corresponded to a temperature of about 590 °C. According to [32], in this temperature range ideal kaolinite begins transforming into metakaolinite with the water of crystallization being removed:



The thermogram presented in Fig. 3 shows an asymmetric peak with an inflection at a temperature of about 620 °C. Such a double peak can be interpreted as an increase in the structural disorder of kaolinite following a decrease in the size of its crystallographic planes, which is characteristic of the formation of metakaolinite. In certain situations, this effect is explained by the presence in the clay of a mineral that is difficult to identify – dickite, whose mineralogical properties are close to those of kaolinite [33]. Thus [34, 35] present a differential thermal analysis of kaolin clay from the Novoorsky deposit, which did not demonstrate asymmetric peaks. At temperatures above 680 °C, no thermal processes were observed, which is characteristic of the state of transformation of kaolinite into metakaolinite [36].

3.3. Morphology of kaolinite particles

Optical images of the particles in transmitted light are given in Fig. 4. In their initial state, the particles are translucent, inhomogeneous, and lamellar (Fig. 4a); their size does not exceed 10 μm. At larger magnification (Fig. 4b), 10±5 μm particles were observed to have kaolinite-like faceting (a hexagon at the end of the crystal).

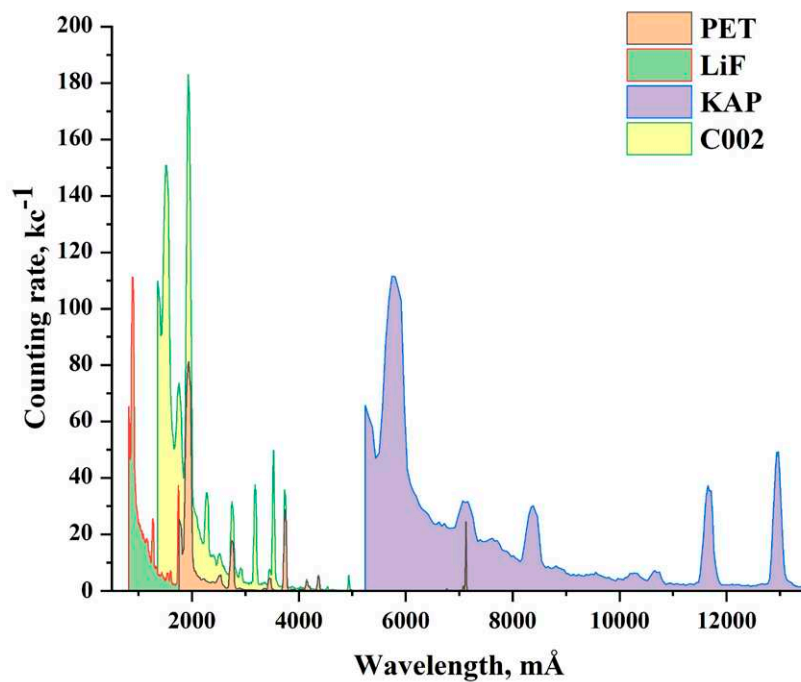


Fig. 2. Integral XRF spectrum of the enriched kaolin clay; PET, LiF, KAP, and C002 are analysing crystals

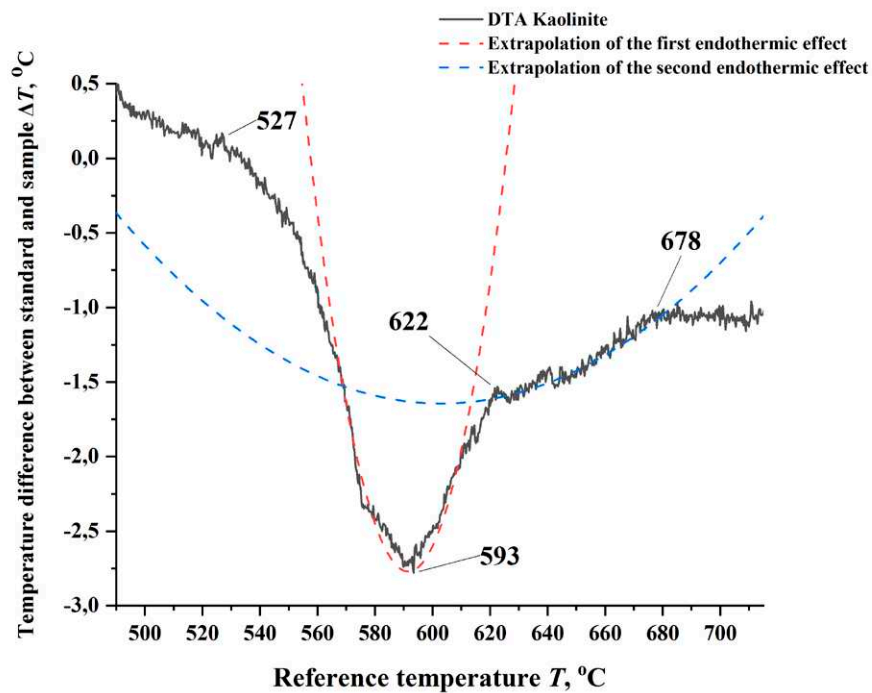


Fig. 3. Derivatogram (thermogram) of the enriched kaolin clay

There were also cleavage planes in certain crystals. According to the modern classification, the analysed clay can be attributed to the 1st class, which corresponds to the presence of minerals with the least defective structures and the least physico-chemical activity [20].

We also performed a comparative morphometric study of kaolinite particles before and after the DTA. After the first endothermic effect of annealing at 620 °C we observed aggregations of particles (Fig. 4c), their partial agglomeration and cluster wafers of up to 30 μm with hexagonal

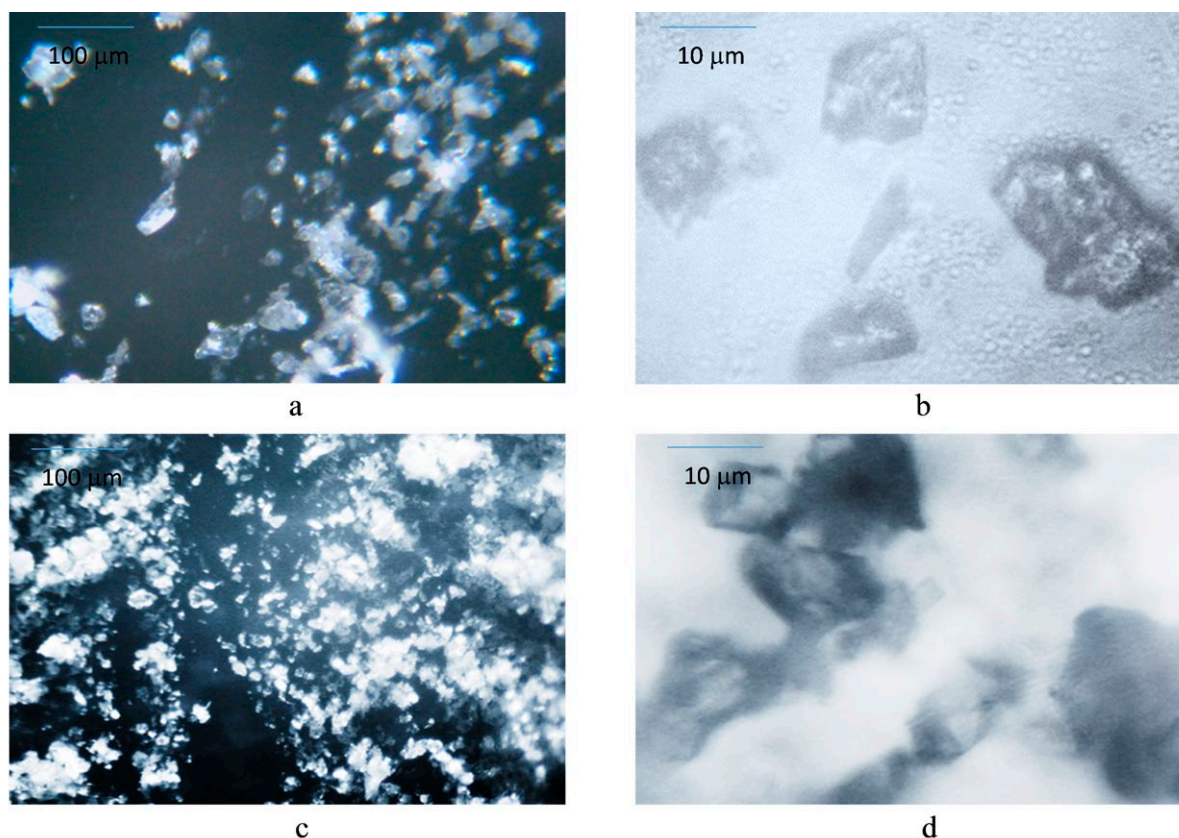


Fig. 4. Lamellar kaolinite particles: a – before thermal treatment (1 cm = 50 μm); b – before thermal treatment (1 cm = 5 μm); c – after thermal treatment (1 cm = 50 μm); d – after thermal treatment (1 cm = 5 μm)

symmetry (Fig. 4d). The formation of point and phase contacts was confirmed by a slight increase in the number of crystalline phases, according to the X-ray phase analysis [8, 18, 19]. A similar microstructure of the products of heating of kaolin clay of the Novoorsky deposit obtained in reflected light is described in [34].

3.4. Interpretation of the IR and Raman spectra (specifying the chemical bonds)

The main purpose the IR spectroscopy was to specify the chemical bonds in the clay sample and the presence of dickite. In order to do this, we obtained the IR and Raman spectra of the samples of enriched kaolin clay (Fig. 5, 6).

The results of the analysis of the IR spectra are given in Table 2. The spectra of the kaolin samples before and after the DTA demonstrate (Fig. 5) that the IR radiation was mainly absorbed in two regions: from 3600 to 3700 cm^{-1} and from 800 to 1200 cm^{-1} . The region near 1000 cm^{-1} in both cases corresponded to asymmetric Si-O vibrations in the structure of aluminosilicates [42]. The

spectrum of the initial kaolin clay demonstrated four intense absorption bands corresponding to O-Si-O and O-Al-O vibrations at 1164, 1113, 1025, and 999 cm^{-1} , as well as two absorption bands corresponding to Al-OH vibrations at 935 and 909 cm^{-1} [37]. Two Si-O-Al bending vibrations in the kaolinite structure were observed at 788 and 750 cm^{-1} [37]. The mode at 687 cm^{-1} is explained by Si-O-Al vibrations where the aluminium ion was replaced by a magnesium ion [37, 39]. In the range from 3600 to 4000 cm^{-1} four peaks were registered at 3690, 3670, 3650, and 3619 cm^{-1} corresponding to the vibrations of OH groups in the kaolinite structure [37, 38]. The above presented data led us to the conclusion that the clay sample contained mainly kaolinite with an insignificant amount of free silica impurities.

The Raman spectra of the enriched kaolin clay are presented in Fig. 6 and Table 3. The Raman spectra of the kaolin clay demonstrated two main regions explained by the absorption by hydroxyl groups in the range from 3000 to 4000 cm^{-1} and by crystalline vibrations in the

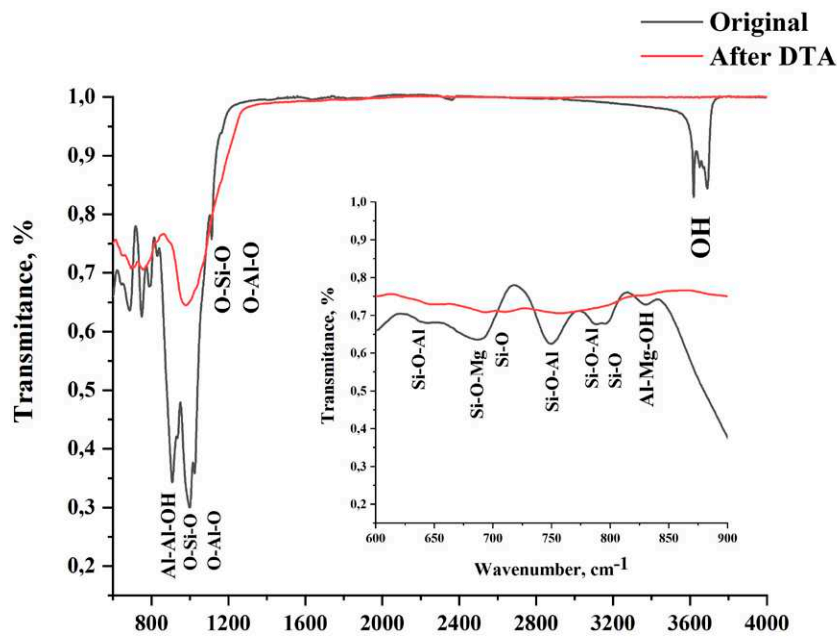


Fig. 5. IR spectra of the samples of enriched kaolin clay before and after DTA

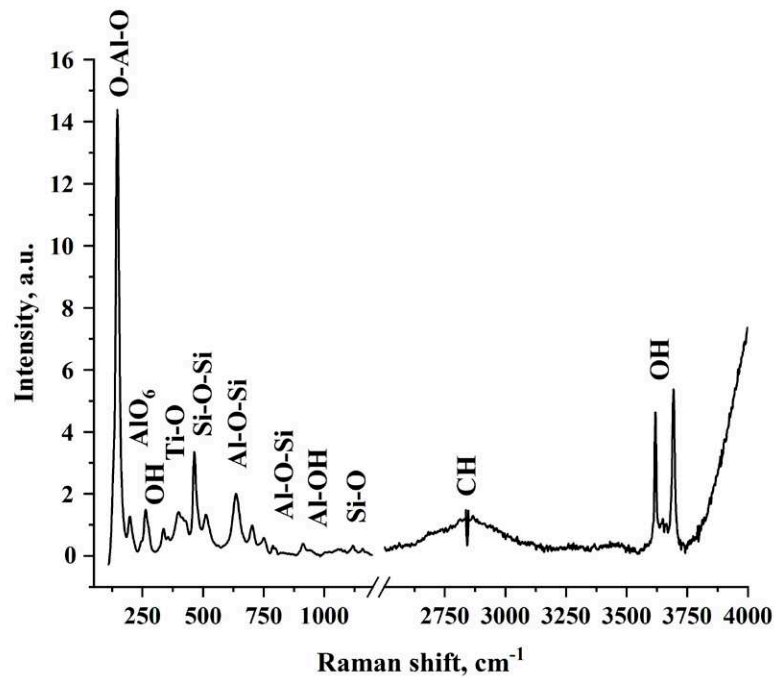


Fig. 6. Raman spectrum of the initial enriched kaolin clay

range of up to 1200 cm^{-1} . The vibration region of hydroxyl groups demonstrated four absorption bands: at 3619, 3648, 3661, and 3693 cm^{-1} . These modes were responsible for the vibrations of constitutional water (OH groups of kaolinite) [46].

In the range from 140 to 1000 cm^{-1} there were a large number of intense absorption bands corresponding to the vibrations of the

crystal structure of kaolinite [43–46]. The Raman spectrum also demonstrated weak absorption bands of quartz [43] and Ti-O chemical bonds [43]. Unfortunately, the intense absorption of kaolinite and partial overlap of the bands makes the identification process rather problematic. The presence of dickite was excluded based on the absence of characteristic Si-O vibration

Table 2. Characteristic modes of interatomic bonds in the samples of enriched kaolin clay in the initial state obtained by means of IR spectroscopy

Wavenumber starting material, cm ⁻¹	Wavenumber after DTA, cm ⁻¹	Oscillation type	Mineral
643	645	Si-O-Al [37, 38]	Kaolinite
687	–	Si-O-Mg [37 - 39]	Kaolinite
-	694	Si-O [40]	Silica
750	760	Si-O-Al [37, 38]	Kaolinite
790	–	Si-O-Al [37, 38]	Kaolinite
797	795	Si-O-Si [40, 19]	Kaolinite
830	830	Al-Mg-OH [37, 38]	Kaolinite
909, 935	–	Al-Al-OH [37, 38, 19]	Kaolinite
1164, 1113, 1025, 999	1164, 1036, 979	O-Si-O, O-Al-O [37, 38, 41]	Kaolinite
3620	–	Constitutional water (OH-group) [37, 38, 19, 41]	Kaolinite
3652, 3670, 3690	–	Constitutional water (OH-group) [37, 38, 41]	Kaolinite

Table 3. Characteristic modes of interatomic bonds in the samples of enriched kaolin clay in the initial state obtained by means of Raman spectroscopy

Raman shift, cm ⁻¹	Oscillation type	Mineral
146,2	O-Al-O [43]	Kaolinite
198	AlO ₆ octahedron [44]	Kaolinite
263	Конституционная вода (OH-группа) [44]	Kaolinite
337	Constitutional water (OH-group) [43]	Kaolinite
355	SiO ₄ tetrahedron [44]	Kaolinite / Silica
413	Ti-O [43]	Substitutional ion in kaolinite
428	Si-O-Si [44]	Kaolinite / Silica
464	Si-O-Si [43]	Silica
512	Al-O-Si [44]	Kaolinite
702	Al-OH [44]	Kaolinite
750	Al-O-Si [44, 43]	Kaolinite
788	Al-O-Si [44, 43]	Kaolinite
800	Al-O-Si [45]	Dickite
911	Al-OH [44, 43]	Kaolinite
1070	Si-O [45]	Dickite
1118	Si-O [45]	Dickite
2836	CH [27]	Organic compounds
3619	Constitutional water (OH-group)	Kaolinite
3648	Constitutional water (OH-group)	Kaolinite
3661	Constitutional water (OH-group)	Kaolinite
3693	Constitutional water (OH-group)	Kaolinite

bands with the peaks at 1070 and 1118 cm^{-1} [45]. A broad weak absorption band with a peak at 2836 cm^{-1} corresponds to C-H vibrations of organic compounds in the clay [27].

After the DTA the clay underwent structural transformations and the IR spectrum did not register the absorption bands corresponding to the vibrations of OH groups (Fig. 4, Table 2). The absence of absorption bands at 3600 cm^{-1} indicates complete dehydration of the crystal structure of kaolinite, i.e. its transformation into metakaolinite. The identification of the spectra of the studied structures was hindered by the partial amorphisation of silicon oxide whose absorption bands overlapped with the absorption bands of anhydrous aluminosilicates. To specify the fine structure, other methods should be used, for instance EPR spectroscopy.

3.5. Paramagnetic centres in the structure of enriched kaolin clay

EPR spectroscopy of soils and nonmetallic minerals is often used to study their structural features [47, 48]. The EPR spectra of mechanically and chemically treated kaolin clay in the initial state and after annealing at 620 °C (for a detailed study of structural transformations) and 900 °C are given in Fig. 7.

The EPR spectrum of the initial clay (Fig. 7A) contained characteristic groups of resonances: the first group of low field lines with the central g -factor of about 4.2 and the second group of overlapping lines in a strong magnetic field with $g \approx 2.0$. Similar to standard kaolinites, the analysed sample demonstrated the following lines: the so-called A-line with $g \approx 4.2$ and three symmetric B-lines of various intensity with $g_{B1} = 4.6790$, $g_{B2} = 4.3173$, and $g_{B3} = 3.7986$. The A-line in a weak magnetic field with $g \approx 4.2$ belonged to Fe^{3+} ions in the crystal lattice with strong trigonal distortions. It is known that Fe^{3+} ions can replace Al^{3+} ions in an octahedral system of phyllosilicates and do not replace Si atoms in the tetrahedral system (Fig. 1) [49]. B-lines are often allowed in the EPR spectra of powders [28]. Their presence indicated that the layers were regularly packed and the mineral had good crystallinity. According to [50] in this triplet, the side lines with $g_{B1} = 4.6790$ and $g_{B3} = 3.7986$ are explained by the replacement of the Fe^{3+} ion, located in the surface layers of kaolinite. It

is known [28, 51] that the ratio of the intensity of lines of the B/A spectrum helps to determine the degree of structural perfection of kaolinite crystals, i.e. the Hinckley crystallinity index. In our study it was close to 0.2.

A broad intense line with $g \approx 2.0$ was identified as a line of magnetic resonance of Fe_3O_4 superparamagnetic particles. Such spectra are also called superparamagnetic resonance (SPR) spectra [52, 53]. The line usually overlaps with signals connected with local defects: narrow lines close to $g \approx 2.0$ [30]. Lines with $g = 2.0016$ and $g = 1.9789$ are explained by electron-hole centres formed as a result of isomorphic substitutions of cations in the octahedral sheet. These are O-centres of the substitution stabilisers $\text{Mg}^{2+} \rightarrow \text{Al}^{3+}$. They are relatively poorly connected with the structure of the mineral and served as indicators of the external influence on the structural order of the mineral.

Annealing of the enriched kaolin clay at 620 °C practically did not change the location, width, or shape of the magnetic resonance line with the g -factor of 2.0018 (Fig. 6b). Therefore, the annealing did not change the concentration of Fe^{3+} ions inside the distorted crystallographic cells, and Fe^{3+} ions did not transform into unobserved Fe^{2+} ions and did not leave the distorted octahedral cell. The width of the low field line with the g -factor of 4.2085 decreased to about 14 mT, and the amplitude increased by three times similar to [53]. A significant increase in the intensity of the isotropic signal with $g = 4.2085$ indicated a decrease in the Hinckley crystallinity index almost to zero and formation of metakaolinite. A prominent connection between the resonance and the degree of perfection of crystals agrees well with the interpretation of the results of the DTA. During the formation of metakaolinite the environment of the Fe^{3+} ions in the kaolinite lattice changed following the modification of Al^{3+} coordination in the octahedral layer of the lattice.

The signal explained by the hole defects (vacancies) caused by the replacement of Al^{3+} ions with double charge ions (in this case, Mg^{2+} , Mn^{2+} , and Fe^{2+}) disappeared. The position and amplitude of the second signal remained the same.

The end of the transformation of the enriched kaolin clay processed at 900 °C into metakaolinite

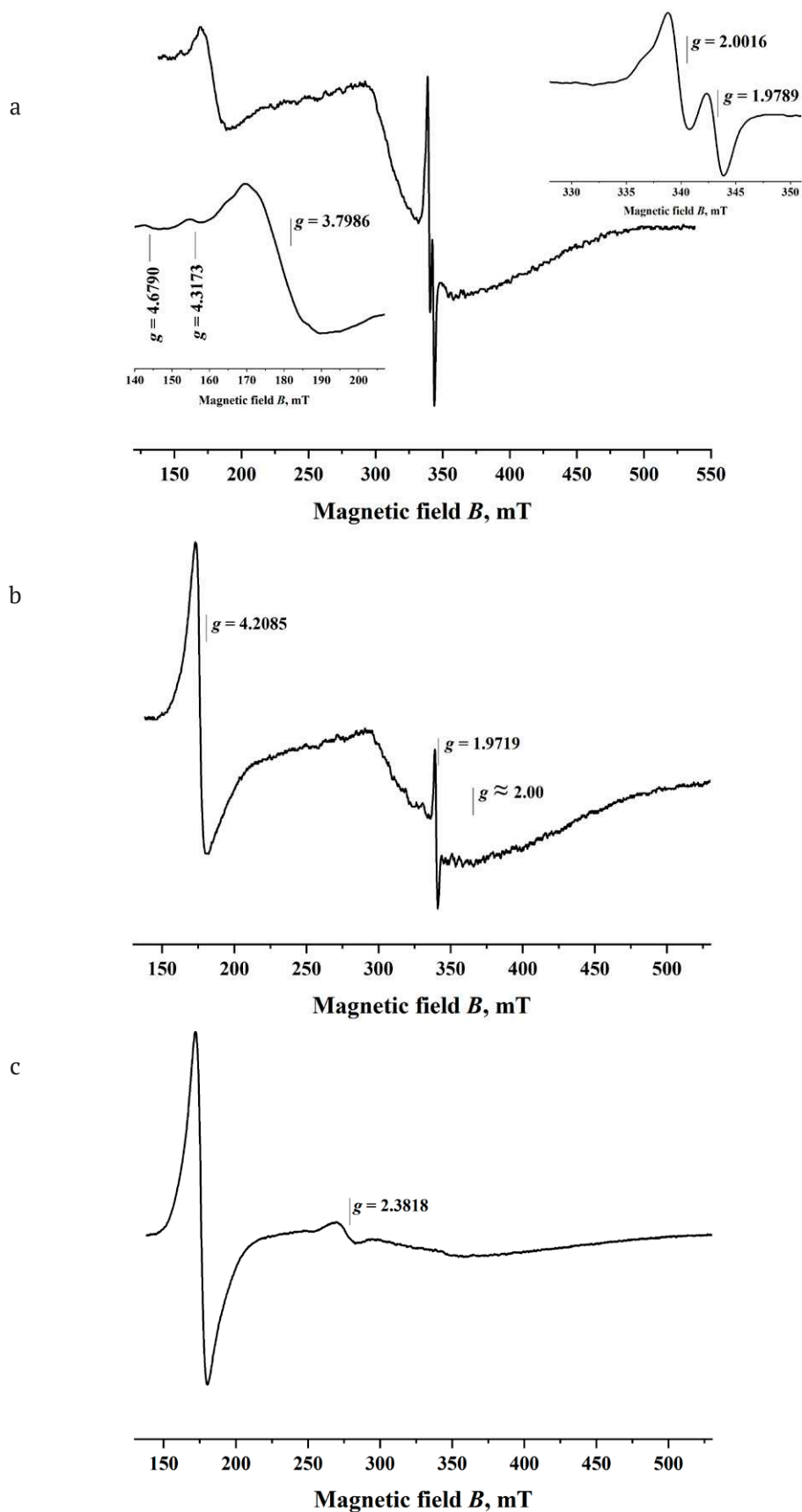
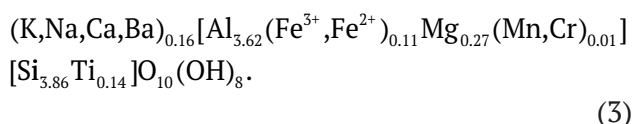


Fig. 7. EPR spectrum of the enriched kaolin clay: a – initial; b – after 620 °C; c – after 900 °C

resulted in a slight expansion of the line with $g \approx 2.00$ and a significant decrease in the amplitude (Fig. 7c). It is possible that, when the crystal lattice was destroyed, the diffusion of Fe^{3+} ions caused the depletion of supermagnetic domains rich in iron, which resulted in a decrease in the concentration of diluted Fe^{3+} [53]. This explains the signal with $g = 2.3819$ which is attributed to the release of aggregated iron Fe^{3+} as a cluster previously contained in ferrihydrite impurities which are not clay minerals [54]. As a rule, the signal is not observed in elutriated clays. Therefore, the analysed sample of enriched kaolin clay requires longer and more thorough chemical treatment in order to extract weakly bound iron ions from the surface layers of kaolinite particles and from impurities.

Manganese and copper lines are indiscernible, presumably due to a low concentration of paramagnetic centres in the sample (less than 0.03%). Titanium lines are also indiscernible, same as in [55, 56], due to correct substitution of $\text{Si}^{4+} \rightarrow \text{Ti}^{4+}$ in the tetrahedral layer. Ca^{2+} , Na^+ , K^+ , and Ba^{2+} cations are usually described as compensator cations and located outside the hydroxyl and siloxane sheets. Al^{3+} cations together with substituting Mg^{2+} , Fe^{3+} , Fe^{2+} , and Mn^{2+} ions are attributed to octahedral positions.

Based on the obtained results, we specified the formula of kaolinite after the mechanical and chemical treatment of the sample:



The corrections in the structural formula agree with the changes in the quantitative and qualitative compositions of the hydroxyl and siloxane sheets of the kaolinite lattice as compared to the averaged formula (1).

4. Conclusions

The XRF determined that the chemical composition of the analysed kaolin clay includes the following oxides: SiO_2 (silica), Al_2O_3 (alumina), Na_2O and K_2O (alkali oxides), Fe_2O_3 and TiO_2 (colouring oxides), as well as CaO (lime), and MgO (magnesia). Trace amounts of barium, sulphur, and chromium registered by the XRF were also registered.

The results of the IR and Raman spectroscopy led us to the conclusion that the clay sample contained mainly kaolinite with an insignificant amount of free silica impurities. The disappearance of the absorption band connected with the vibrations of the OH groups on the IR spectrum of the clay after DTA indicates complete dehydration of the crystal structure of kaolinite, i.e. its transformation into metakaolinite. The EPR spectroscopy registered the introduction of iron ions into the octahedral sheet of the kaolinite lattice.

The study specified the structural formula of kaolinite from the Koskolsky deposit in the Orenburg Region using a series of experiments. Thus, we assessed the substance used as a raw material in ceramics industry. The study determined that spectroscopic methods can be used to analyse fine structural parameters, namely the degree of crystallinity and the mechanism of introduction of iron ions. We also monitored the process of metakaolinitisation as a result of dehydration of kaolinite by means of IR, Raman, and EPR spectroscopy and the DTA.

Author contributions

A. G. Chetverikova – research concept, analysis of the results, analysis of the EPR spectroscopy, deriving the structural formula, text writing and editing. V. N. Makarov – analysis of the results, DTA analysis, graphs plotting, text writing and editing. O. N. Kanygina – analysis of the results, methodology development, analysis of the particles morphology, text writing and editing. M. M. Seregin – analysis of the IR and Raman spectroscopy. E. A. Stroganova – X-ray fluorescence analysis and Raman spectroscopy.

Conflict of interests

The authors declare that they have no known competing financial interests or personal relationships that could have influenced the work reported in this paper.

References

1. Grevtsev V. A., Lygina T. Z. Morphological and structural features of natural, activated and synthesized substances*. *Bulletin of the Kazan Technological University*. 2010;(8): 236–249. (in Russ.). Available at: <https://www.elibrary.ru/item.asp?id=15240366>
2. Klepikov M. S. *Study of the physicochemical properties of kaolins from the Poletaevsky deposit of the*

*Chelyabinsk region and ceramic materials based on them**. Cand. chem. sci. diss. Abstr. Chelyabinsk: 2012. 23 p. (in Russ.). Available at: <https://www.dissercat.com/content/issledovanie-fiziko-khimicheskikh-svoystv-kaolinov-poletaevskogo-mestorozhdeniya-chelyabinsk>

3. Vereshchagin V. I., Shatalov P. I., Mogilevskaya N. V. Speckless technology of diopside ceramic dielectrics based on iron-free diopside raw materials from the Slyudyanskoye deposit*. *Refractories and Industrial Ceramics*. 2006;(8): 33–35. (in Russ.). Available at: <https://www.elibrary.ru/item.asp?id=16501015>

4. Worasith N., Goodman B. A., Neampan J., Jeyachoke N., Thiravetyan P. Characterization of modified kaolin from the Ranong deposit Thailand by XRD, XRF, SEM, FTIR and EPR techniques. *Clay Minerals*. 2011;46(4): 539–559. <https://doi.org/10.1180/claymin.2011.046.4.539>

5. García-Tojal J., Iriarte E., Palmero S., ... Muñiz P. Phyllosilicate-content influence on the spectroscopic properties and antioxidant capacity of Iberian Cretaceous clays. *Spectrochimica Acta Part A: Molecular and Biomolecular Spectroscopy*. 2021;(251): 119472. <https://doi.org/10.1016/j.saa.2021.119472>

6. Chen J., Min Fan-fei, Liu Ling-yun, Jia Fei-fei. Adsorption of methylamine cations on kaolinite basal surfaces: A DFT study. *Physicochemical Problems of Mineral Processing*. 2020;56(2): 338–349. <https://doi.org/10.37190/ppmp/117769>

7. Worasith N., Ninlaphurk S. Mungpayaban H., Wen D., Goodman B. Characterization of paramagnetic centres in clay minerals and free radical surface reactions by EPR spectroscopy. 2014. Available at: <https://www.researchgate.net/publication/292536710>

8. Chetverikova A. G., Kanygina O. N., Filyak M. M. *Structural transformations in oxides constituting natural clays under the influence of a microwave field**. Orenburg: OGU Publ.; 2021. 204 p. (in Russ.)

9. Nasirov R. N., Samatov I. B., Slyussarev A. P., Nasirov A. R. Complex mineralogical and lithological study of sedimentary oil and gas bearing rocks of the precaspian region by EPR, IR-spectroscopy, X-ray diffractometry and thermal analysis*. *News of the national academy of sciences of the republic of Kazakhstan series of geology and technical sciences*. 2018;(4): 174–185. (In Russ.). Available at: <http://geolog-technical.kz/images/pdf/g20184/174-185.pdf>

10. Rutherford D. W., Chiou C. T., Eberl D. D. Effects of exchanged cation on the microporosity of montmorillonite. *Clays and Clay Minerals*. 1997;45(4): 534–543. <https://doi.org/10.1346/ccmn.1997.0450405>

11. Balan E., Allard T., Boizot B., Morin G., Muller J. P. Quantitative measurement of paramagnetic Fe³⁺ in kaolinite. *Clays and Clay Minerals*. 2000;48(4): 439–445. <https://doi.org/10.1346/ccmn.2000.0480404>

12. Gaité J. M., Ermakoff P., Allard T., Müller J. P. Paramagnetic Fe³⁺: a sensitive probe for disorder in kaolinite. *Clays and Clay Minerals*. 1997;45(4): 496–505. <https://doi.org/10.1346/CCMN.1997.0450402>

13. Dobosz B., Krzymiński R. Characteristic of paramagnetic centres in burnt clay and pottery by the EPR method. *Radiation measurements*. 2007;42(2): 213–219. <https://doi.org/10.1016/j.radmeas.2006.11.003>

14. Goodman B. A., Worasith N., Deng W. EPR spectra of a new radiation-induced paramagnetic centre in kaolins. *Clay Minerals*. 2016;51(5): 707–714. <https://doi.org/10.1180/claymin.2016.051.5.01>

15. Chibilev A. A., Petrishchev V. P., Klimentiev A. I., ... Rychko O. K. *Geographical atlas of the Orenburg region**. Moscow: DIK Publ.; 1999. 96 p. (in Russ.)

16. Kadyrbakov I. Kh., Isinbaev A. V., Zubairov R. R. Structural features of eluvial kaolin deposits of the Kovylnoe deposit in the Orenburg region (according to exploration results)*. *Practice of geologists in production. Proceedings of the VI All-Russian Student Scientific and Practical Conference dedicated to the Year of Science and Technology. Rostov-on-Don – Taganrog, 2021*. Rostov-on-Don: Southern Federal University Publ.; 2021. p. 36–38. (in Russ.)

17. Vasyanov G. P., Gorbachev B. F., Chechulina Yu. V., Shmelkov N. T. Deposit eluvial kaolin Kovylny in the east of the Orenburg region. *National Geology (Otechestvennaya Geologiya)*. 2012;(4): 11–19. (in Russ., abstract in Eng.). Available at: <https://www.elibrary.ru/item.asp?id=17789124>

18. Kanygina O. N., Chetverikova A. G., Alpysbaeva G. Zh., ... Gun'kov, V. V. Characteristics of kaolin clay from the deposit in the svetlinskii area of Orenburg oblast. *Glass and Ceramics*. 2021;77(9-10): 355–360. <https://doi.org/10.1007/s10717-021-00306-y>

19. Chetverikova A. G., Kanygina O. N., Alpysbaeva G. Z., Yudin A. A., Sokabayeva S. S. Infrared spectroscopy as the method for determining structural responses of natural clays to microwave exposure. *Condensed Matter and Interphases*. 2019;21(3): 446–454. <https://doi.org/10.17308/kcmf.2019.21/1155>

20. Osipov V. I., Sokolov V. N. *Clays and their properties. Composition, structure and formation of properties**. Moscow: Geos Publ.; 2013. 578 p. (In Russ.)

21. GOST 21216-2014. Clay material. Test methods: approved and put into effect by the Interstate Council for Standardization, Metrology and Certification (minutes of May 25, 2014 No. 45-2014): introduction date 2015-07-01. (in Russ.) Available at: <https://docs.cntd.ru/document/1200115068>

22. Chetverikova A. G., Chetverikova D. K. Transduction of crystal chemistry methods into the physics of materials*. *University complex as a regional center of education, science and culture. Collection of*

materials of the All-Russian Scientific and Methodological Conference, Orenburg, January 26–27, 2022. Orenburg: Orenburg State University Publ.; 2022. p. 2939–2942. (In Russ.)

23. ISO 21822:2019(en). Fine ceramics (advanced ceramics, advanced technical ceramics). Measurement of iso-electric point of ceramic powder*. This document was prepared by Technical Committee ISO/TC 206, Fine ceramics. Available at: <https://www.iso.org/obp/ui>

24. Chetverikova A. G. Determination of particle size distribution and electrokinetic potential of phyllosilicate powders by photon correlation spectroscopy. *Measurement Techniques*. 2022;64(11): 936–941. <https://doi.org/10.1007/s11018-022-02024-5>

25. ISO 24235:2007(en). Fine ceramics (advanced ceramics, advanced technical ceramics). Determination of particle size distribution of ceramic powders by laser diffraction method. ISO 24235 was prepared by Technical Committee ISO/TC 206, Fine ceramics. Available at: <https://www.iso.org/obp/ui>

26. GOST 9169-2021. Clay raw materials for the ceramic industry. Classification: adopted by the Interstate Scientific and Technical Commission for Standardization, Technical Regulation and Conformity Assessment in Construction (MNTKS) (Minutes of June 30, 2021 № 141-P): introduction date 2022-04-01. (In Russ.) Available at: https://allgosts.ru/81/060/gost_9169-2021

27. Becker Yu. *Spectroscopy*. Moscow: Technosphere Publ.; 2009. 528 p. (in Russ.)

28. Hall P. L. The application of electron spin resonance spectroscopy to studies of clay minerals: I. Isomorphous substitutions and external surface properties. *Clay Minerals*. 1980;15(4): 321–335. <https://doi.org/10.1180/claymin.1980.015.4.01>

29. Bortnikov N. S., Mineeva R. M., Savko A. D., ... Speransky A. V. Kaolinite history in the weathering crust and associated clay deposits: EPR data. *Doklady Earth Sciences*. 2010;433: 927–930. <https://doi.org/10.1134/S1028334X10070184>

30. Babinska J., Dyrek K., Wyszomirski P. EPR study of paramagnetic defects in clay minerals. *Mineralogia*. 2007;38(2): 125. <https://doi.org/10.2478/v10002-007-0021-x>

31. Liu Y., Huang Q., Zhao L., Lei S. Influence of kaolinite crystallinity and calcination conditions on the pozzolanic activity of metakaolin. *Gospodarka Surowcami Mineralnymi-Mineral Resources Management*. 2021: 39–56. <https://doi.org/10.24425/gsm.2021.136295>

32. Escalera E., Antti M.L., Odén M. Thermal treatment and phase formation in kaolinite and illite based clays from tropical regions of Bolivia. *IOP Conference Series: Materials Science and Engineering*. *IOP Publishing*. 2012;31(1): <https://doi.org/10.1088/1757-899X/31/1/012017>

33. Stoch L. Significance of structural factors in dehydroxylation of kaolinite polytypes. *Journal of Thermal Analysis and Calorimetry*. 1984;29(5): 919–931. <https://doi.org/10.1007/bf02188838>

34. Guryeva V.A. Physico-chemical studies of the use of dunites in decorative and finishing ceramics. Orenburg: IPK GOU OGU: 2007. 129 p. (in Russ.)

35. Rakhimov R.Z., Rakhimova N.R., Gaifullin A.R., Morozov V.P. Dehydration of clays of different mineral composition during calcination. *Izvestiya KGASU*. 2016;4(38): 388–394. (in Russ.)

36. Janotka I., Puertas F., Palacios M., Kuliffayová M., Varga C. Metakaolin sand-blended-cement pastes: Rheology, hydration process and mechanical properties. *Construction and Building Materials*. 2010;24(5): 791–802. <https://doi.org/10.1016/j.conbuildmat.2009.10.028>

37. Tironi A., Trezza M.A., Irassar E.F., Scian A.N. Thermal treatment of kaolin: effect on the pozzolanic activity. *Procedia Materials Science*. 2012;(1): 343–350. <https://doi.org/10.1016/j.mspro.2012.06.046>

38. Khang V.C., Korovkin M.V., Ananyeva L.G. Identification of clay minerals in reservoir rocks by FTIR spectroscopy. *IOP Conference Series: Earth and Environmental Science*. *IOP Publishing*. 2016;43(1): 012004.

39. Rosa M.S.L., Silva R.A.O., Sousa P.E., do Nascimento R.T., Knoerzer T., Santos M.R.M.C. Doxazosin adsorption in natural, expanded, and organophilized vermiculite-rich clays. *Cerâmica*. 2022;68(385): 75–83. <https://doi.org/10.1590/0366-69132022683853175>

40. Fricke H.H., Mattenklott M., Parlar H., Hartwig A. Method for the determination of quartz and cristobalite [Air Monitoring Methods, 2015]. *The MAK – Collection for Occupational Health and Safety: Annual Thresholds and Classifications for the Workplace*. 2002;1(1): 401–436. <https://doi.org/10.1002/3527600418.am0sio2fste2015>

41. Tosoni S., Doll K., Ugliengo P. Hydrogen bond in layered materials: structural and vibrational properties of kaolinite by a periodic B3LYP approach. *Chemistry of Materials*. 2006;18(8): 2135–2143.

42. Jovanovski G., Makreski P. Minerals from macedonia. XXX. Complementary use of vibrational spectroscopy and x-ray powder diffraction for spectro-structural study of some cyclo-, phyllo- and tectosilicate minerals. A review. *Macedonian Journal of Chemistry and Chemical Engineering*. 2016;35(2): 125–155. <https://doi.org/10.20450/mjcc.2016.1047>

43. Saikia B.J., Parthasarathy G., Borah, R.R., Borthakur R. Raman and FTIR spectroscopic evaluation of clay minerals and estimation of metal contaminations in natural deposition of surface sediments from Brahmaputra river. *International Journal of Geosciences*, 2016;7(7): 873–883.

44. Samyn, P., Schoukens, G., Stanssens, D. Kaolinite nanocomposite platelets synthesized by intercalation and imidization of poly (styrene-co-maleic anhydride). *Materials*. 2015;8(7): 4363–4388. <https://doi.org/10.3390/ma8074363>
45. Johnston C.T., Helsen J., Schoonheydt R.A., Bish D.L., Agnew S.F. Single-crystal Raman spectroscopy study of dickite. *American Mineralogist*. 1998;83(1-2): 75–84. <https://doi.org/10.2138/am-1998-1-208>
46. Basu A., Mookherjee M. Intercalation of Water in Kaolinite ($\text{Al}_2\text{Si}_2\text{O}_5(\text{OH})_4$) at Subduction Zone Conditions: Insights from Raman Spectroscopy. *ACS Earth and Space Chemistry*. 2021;5(4): 834–848. <https://doi.org/10.1021/acsearthspacechem.0c00349>
47. Vasilevich R. S., Beznosikov V. A., Lodygin E. D. Molecular structure of humic substances in permafrost hilly peatlands of the forest-tundra. *Soil science*. 2019;(3): 317–329. (in Russ.) <https://doi.org/10.1134/S0032180X19010167>
48. Kurochkina G. N., Kerzhentsev A. S., Sokolov O. A. Physico-chemical study of soils contaminated with rocket fuel components. *Soil science*. 1999;(3): 359–369. (in Russ.)
49. Calas G. Electron paramagnetic resonance. In *Spectroscopic Methods in Mineralogy and Geology* (F.C. Hawthorne, Eds.). *Reviews in Mineralogy*. 1988;(1): 513–571.
50. Savko A. D., Krainov A. V., Ovchinnikova M. Yu., Milash A. V., Novikov V. M. Ages of formation of weathering crusts and connection with them of deposits of secondary kaolins and ceramic clays in the Phanerozoic of the Voronezh anticline. *Bulletin of the Voronezh State University. Series: Geology*. 2019;(3):23–34. (in Russ.)
51. Grevtsev V.A., Lygina T.Z. Aspects of application of the method of electron paramagnetic resonance in the study of non-metallic raw materials. *Exploration and protection of mineral resources*. 2010;(8): 34–39. (in Russ.)
52. Slay D., Cao D., Ferré E.C., Charilaou M. Ferromagnetic resonance of superparamagnetic nanoparticles: The effect of dipole–dipole interactions. *Journal of Applied Physics*. 2021;130(11): 113902. <https://doi.org/10.1063/5.0060769>
53. Bertolino L.C., Rossi A.M., Scorzelli R.B., Torem M.L. Influence of iron on kaolin whiteness: An electron paramagnetic resonance study. *Applied Clay Science*. 2010;49(3): 170–175. <https://doi.org/10.1016/j.clay.2010.04.022>
54. Lyutoev V.P., Burtsev I.N., Saldin V.A., Golovataya O.S. EPR and IR spectroscopy of oil shale: material composition and forms of localization of heavy metals (Chim-Loptyugskoye deposit, Komi Republic). *Mineralogy of technogenesis*. 2012;(13): 115–132. (in Russ.)
55. Gaité J. M., Ermakoff P., Muller J. P. Characterization and origin of two Fe^{3+} EPR spectra in kaolinite. *Physics and Chemistry of Minerals*. 1993;20(4): 242–247.
56. Djemai A., Balan E., Morin G., Hernandez G., Labbe J.C., Muller J.P. Behavior of paramagnetic iron during the thermal transformations of kaolinite. *Journal of the American Ceramic Society*. 2001;84(5): 1017–1024. <https://doi.org/10.1111/j.1151-2916.2001.tb00784.x>

* Translated by author of the article.

Information about the authors

Anna G. Chetverikova, Cand. Sci. (Phys.-Math.), Associate Professor, Dean of the Physics Faculty, Orenburg State University (Orenburg, Russian Federation).

<https://orcid.org/0000-0002-7045-3588>
kr-727@mail.ru

Valery N. Makarov, Cand. Sci. (Phys.-Math.), Senior Lecturer, Department at Physics and Methods of Teaching Physics, Orenburg State University (Orenburg, Russian Federation).

<https://orcid.org/0000-0001-5749-1427>
makarsvet13@gmail.com

Olga N. Kanygina, Dr. Sci. (Phys.-Math.), Full Professor, Department of Chemistry, Orenburg State University (Orenburg, Russian Federation)

<https://orcid.org/0000-0001-6501-900X>
onkan@mail.ru

Mikhail M. Seregin, Analytical Chemist, Lumex-Centrum LLC (Moscow, Russian Federation).

<https://orcid.org/0000-0002-2263-9679>
Sereginmm@lumex.ru

Elena A. Stroganova, Cand. Sci. (Chem.), Associate Professor of the Department of Chemistry, Orenburg State University (Orenburg, Russian Federation).

<https://orcid.org/0000-0002-6583-516X>
stroganova_helen@mail.ru

Received 21.10.2022; approved after reviewing 20.12.2022; accepted for publication 15.01.2023; published online 25.06.2023.

Translated by Yulia Dymant

Edited and proofread by Simon Cox